THE ASTROPHYSICAL JOURNAL, 465:312–326, 1996 July 1

HOT ONE-TEMPERATURE ACCRETION FLOWS AROUND BLACK HOLES

ANN A. ESIN, RAMESH NARAYAN, AND EVE OSTRIKER
Harvard-Smithsonian Center for Astrophysics, Cambridge, MA 02138
AND
INSU YI
Institute for Advanced Study, Princeton, NJ 08540
Received 1995 November 20; accepted 1996 January 17

ABSTRACT

We describe hot, optically thin solutions for one-temperature accretion disks around black holes. We include cooling by synchrotron, bremsstrahlung, and Comptonization. Our solutions are thermally and viscously stable, with gas temperatures on the order of $T \sim 10^9$–$10^{10.7}$ K. The thermal stability is a direct result of the inclusion of synchrotron cooling.

The new solution branch is related to the advection-dominated solution for a two-temperature gas, described by Narayan & Yi (1995b). It is present only for mass accretion rates less than some critical $\dot{M}_{\rm crit}$, which depends on the radius R and viscosity parameter α. The solutions are advection dominated for extremely low values of $\dot{M}$. However, for a range of intermediate accretion rates, the new solutions are both hot ($T \sim 10^{10}$ K) and cooling dominated. Because of this new feature, one-temperature solutions are significantly more luminous than the corresponding two-temperature solutions at the same $\dot{M}$.

The radial profile of the new solutions is unusual. The inner parts of the flow are cooling-dominated and have a disklike geometry, while the outer parts are fully advection-dominated and nearly quasi-spherical.

Subject headings: accretion, accretion disks — black hole physics — radiation mechanisms: thermal

1. INTRODUCTION

The best known model of an accretion flow is the standard thin accretion disk developed by Shakura & Sunyaev (1973), Novikov & Thorne (1973), and Lynden-Bell & Pringle (1974) (see, for a detailed discussion, Frank, King, & Raine 1992). The basic assumption of the model is that the accreting gas is cool compared to the local virial temperature, so that the flow acquires a thin disk configuration. The disk parameters are calculated assuming an equilibrium between the viscous energy generation inside the disk and radiative cooling from the surface; the latter is computed under the assumption that the disk is optically thick in the vertical direction.

The thin disk model has been widely and successfully used for modeling various low-energy systems, such as accreting white dwarfs and pre–main-sequence stars (Frank et al. 1992). However, the model has had less success explaining the characteristics of relativistic objects such as accreting black holes. There are essentially two problems:

1. In a system containing an accreting black hole, the accretion disk must extend inward to the Schwarzschild radius, $R_{\rm Schw}$. However, for reasonable mass accretion rates and the standard α viscosity prescription, the Lightman-Eardley instability (Lightman & Eardley 1974) causes a breakdown of the thin disk configuration in the inner regions. Therefore, there is some doubt that a thin accretion disk can exist at all close to a black hole.
2. Even if a thin disk is viable, there is a problem with the spectrum. Since the gas in a thin disk model is optically thick, we would expect a roughly blackbody-like spectrum at the high-frequency end, with a cutoff at several keV. However, extensive observations of black hole systems by *Ginga*, *Granat*, and the *Compton Gamma Ray Observatory* (Tanaka 1989; Grebenev et al. 1993; Maisack et al. 1993; Harmon et al. 1994; Johnson et al. 1994; Kinzer et al. 1994; Gilfanov et al. 1995) have made it clear that the spectra of most black hole accretors have hard power-law components extending to a few times 100 keV. This component has to be radiated by an optically thin plasma with temperature $T \gtrsim 10^9$ K. The required temperature is at least an order of magnitude higher than that predicted by the standard thin disk model.

Shapiro, Lightman, & Eardley (1976, hereafter SLE) discovered a new class of solutions at sub-Eddington accretion rates, where the accretion flow is optically thin and quite hot ($T_e \sim 10^8$–10^9 K). These authors also introduced the important idea of a two-temperature plasma in which ions are much hotter than electrons. Since the SLE solution has exactly the necessary characteristics (optically thin hot gas) to explain the spectra of accreting black holes, it has been widely studied and applied in models of X-ray binaries and active galactic nuclei (e.g., Kusunose & Takahara 1985, 1989; White & Lightman 1989; Wandel & Liang 1991; Melia & Misra 1993; Luo & Liang 1994). Unfortunately, the SLE solution is thermally unstable (Pringle, Rees, & Pacholczyk 1973; Piran 1978). The efficiency of bremsstrahlung cooling in the optically thin gas is proportional to the particle density, which decreases with increasing temperature. Therefore, as the gas is perturbed to a higher temperature, the rate of cooling per unit mass decreases, and the gas heats up even further in a runaway process. The thermal instability of the SLE solution makes it unlikely that real flows can take up this configuration.

Recently, a new class of two-temperature advection-dominated solutions has been discovered (Narayan & Yi 1994, 1995a, b; Abramowicz et al. 1995; Chen 1995; Chen et al. 1995). These advection-dominated solutions are optically thin, are hotter even than the SLE solution, and are viscously and thermally stable to large wavelength perturbations (Abramowicz et al.

1995; Narayan & Yi 1995b). Although Kato, Abramowicz, & Chen (1996) have discovered an instability in these flows at short wavelengths, they show that the mode amplitude does not grow significantly, and so the viability of the solutions is not in doubt. The advection-dominated model has been fairly successful in explaining a number of low-luminosity systems (e.g., a model for Sagittarius A* by Narayan, Yi, & Mahadevan 1995; a model for the soft X-ray transient A0620-00 by Narayan, McClintock & Yi 1996; and a model for the central source in NGC 4258 by Lasota et al. 1996) and is, perhaps, also a reasonable model for more luminous systems (Narayan 1996; Narayan, Yi, & Mahadevan 1996).

The most detailed advection-dominated models considered so far are based on a two-temperature plasma that cools through bremsstrahlung, synchrotron, and Comptonization processes. However, there have been discussions in the literature questioning whether a two-temperature plasma can occur at all in astrophysical accretion flows (Phinney 1981; Rees et al. 1982). Begelman & Chiueh (1988) identified a particular mechanism involving collective plasma waves, which may under certain conditions pump energy directly into the electrons and bring the ions and electrons into thermal equilibrium. Therefore, an important question is the following: are there stable hot solutions, analogous to the two-temperature advection-dominated solution, if the plasma is well coupled and has a single temperature for the ions and electrons? Abramowicz et al. (1995) and Chen (1995) did consider single-temperature plasmas in their studies of advection-dominated flows, but they included only bremsstrahlung cooling. As yet, one-temperature models with a more detailed cooling, including synchrotron radiation and Comptonization of synchrotron and bremsstrahlung photons, has not been considered, even though at $T \sim 10^{10}$ K, with an equipartition magnetic field, these processes completely dominate over pure bremsstrahlung cooling. This is the study we present here.

In § 2, we derive the equations that describe an accreting one-temperature plasma. Then we present the main results of the paper in § 3. We find that, as in the two-temperature case (Narayan & Yi 1995b, hereafter NY), the equations allow three branches of solutions: the standard thin Shakura & Sunyaev disk; a hot, optically thin, thermally unstable solution, which is equivalent to the SLE branch for a two-temperature plasma; and, finally, a new hotter and thermally stable disk solution. We describe the properties of the new solution and compare it to the corresponding two-temperature solution branch. Among other things, we find that the one-temperature solution is hotter than the equivalent two-temperature one and is *not* advection-dominated for a wide range of accretion rates. This means that for a given $\dot{M}$, the one-temperature disk is considerably more luminous. We conclude in § 4 with a summary and discussion.

2. BASIC EQUATIONS

2.1. *One-Temperature Accretion Flow*

Narayan & Yi (1994, 1995b) derived a set of local equations describing a vertically averaged, axisymmetric, two-temperature advection-dominated flow. Here we slightly modify these equations by setting the electron and ion temperatures equal to each other. We also include radiation pressure, which NY neglected.

The vertically averaged pressure p and density ρ of the accreting gas are given by

$$p = \rho c_s^2 , \qquad \rho = \frac{\dot{M}}{4\pi R H |v|} , \tag{1}$$

where c_s is the local isothermal sound speed, $\dot{M}$ is the mass accretion rate, R is the radius, H is the vertical scale height of the disk, and v is the radial velocity. We write the total pressure as the sum of the gas, radiation, and magnetic pressures, $p = p_g + p_r + p_m$, and we define three quantities that describe their relative magnitudes: $\beta = p_g/p$ determines the fraction of the total pressure due to gas pressure; $\beta_m = (p_r + p_g)/p = 1 - p_m/p$ determines the importance of magnetic field pressure; finally, χ is defined in such a way that $\beta = \chi\beta_m$, thus χ represents the ratio of gas pressure to the sum of gas and radiation pressure, $\chi = p_g/(p_g + p_r)$. For $\chi \sim 1$ radiation pressure is unimportant, and for $\chi \ll 1$ radiation pressure dominates over gas pressure. In our calculations, we fix the value of β_m, typically at 0.5 corresponding to magnetic pressure equal to 50% of the total pressure, and then solve for χ and β.

With the above definitions, the scaled relations derived by NY take the following form:

$$\begin{aligned}
v &= -2.12 \times 10^{10} \frac{\alpha c_1}{\sqrt{r}} \text{ cm s}^{-1} , \\
c_s^2 &= 4.5 \times 10^{20} \frac{c_3}{r} \text{ cm}^2 \text{ s}^{-2} , \\
\rho &= 3.79 \times 10^{-5} \frac{\dot{m}}{\alpha c_1 m \sqrt{c_3 r^3}} \text{ g cm}^{-3} , \\
B &= 6.55 \times 10^{8} \sqrt{\frac{(1-\beta_m)\dot{m}}{\alpha c_1 m} \left(\frac{c_3}{r^5}\right)^{1/2}} \text{ G} , \\
f &= \frac{1}{\epsilon'} \left(\frac{5/3 - \gamma}{\gamma - 1}\right) , \qquad \gamma = \frac{32 - 24\beta - 3\beta^2}{24 - 21\beta} , \\
q^+ &= 1.84 \times 10^{21} \frac{\epsilon' \dot{m} \sqrt{c_3}}{m^2 r^4} \text{ ergs cm}^{-3} \text{ s}^{-1} .
\end{aligned} \tag{2}$$

Here B is the magnetic field strength and f determines the degree to which the flow is advection dominated. The quantity f ranges from 0 to 1; the limit of $f = 1$ corresponds to the extreme case in which all the energy is stored in the gas as entropy, while $f \to 0$ corresponds to a standard cooling-dominated disk in which most of the generated energy is radiated locally. The quantity q^+ is the viscous dissipation of energy per unit volume, and the factors ϵ', c_1, and c_3 are given by

$$\epsilon' = \frac{1}{2}\left[\left(\frac{18\alpha^2 - x^2}{2x}\right) - 5\right], \qquad x = \frac{9c_3\alpha^2}{2},$$
$$c_1 = \frac{3}{2}c_3, \tag{3}$$
$$c_3 = 3.12 \times 10^{-13}\frac{Tr}{\beta}.$$

In the above equations, masses are scaled in units of the solar mass

$$M = m\,M_\odot;$$

accretion rates are scaled in Eddington units

$$\dot{M} = \dot{m}\dot{M}_{\rm Edd}, \qquad \dot{M}_{\rm Edd} = \frac{L_{\rm Edd}}{\eta_{\rm eff}c^2} = \frac{4\pi GM}{\eta_{\rm eff}\kappa_{\rm es}c} = 1.39 \times 10^{18} m \text{ g s}^{-1},$$

where $\kappa_{\rm es} = 0.4$ cm^2 g^{-1} and we assume the standard efficiency factor $\eta_{\rm eff} = 0.1$ (e.g., Frank et al. 1992); and radii are scaled in Schwarzschild units

$$R = rR_{\rm Schw}, \qquad R_{\rm Schw} = \frac{2GM}{c^2} = 2.95 \times 10^5 m \text{ cm}.$$

If we choose the values of r, m, $\dot{m}$, α, and β_m, and assume specific values for β and T, equations (1), (2), and (3) yield all the other disk parameters.

2.2. *Electron-Positron Pair Equilibrium*

Some of the hot solutions we calculate in this paper have temperatures of up to 10^{10}–10^{11} K (see Fig. 6*d*), and it therefore becomes necessary to include in our model the effects of relativistic pair production and annihilation. Since a complete solution of the pair balance problem is beyond the scope of our calculation, we make some simplifying assumptions.

Svensson (1982, 1984) has explored the properties of pair equilibria in a uniform relativistic plasma in which photons are generated through pair annihilation and bremsstrahlung. He finds that, for temperatures below a certain critical value T_c, there are two equilibrium branches available that are characterized by the ratio z of the pair number density, n_+, to the number density of protons, $n_p = n_e - n_+$: (1) an optically thin low-z branch ($z \ll 1$) in which pair production is dominated by particle-particle processes, and (2) a high-z branch ($z \geq 1$) in which the Thomson scattering optical depth is of order unity and photon-photon pair production dominates. We confine our calculations to the low-z branch, where only particle-particle processes are important. Svensson has shown that the electron-electron pair production rate is always a factor of ~ 10 larger than the electron-proton rate. This allows us to ignore the contribution from electron-proton collisions.

With the above simplifications, we can solve for the equilibrium pair density, z, analytically at any given temperature. For a thermal distribution of electrons and positrons, the pair annihilation rate per unit volume is (Svensson 1982):

$$(\dot{n}_+)_{\rm ann} = \pi c r_e^2 n_e n_+ g(\theta), \tag{4}$$

where $\theta = kT/m_e c^2$ is the dimensionless electron temperature, $r_e = e^2/mc^2$, and $g(\theta)$ is given by

$$g(\theta) = \left\{1 + \left[\frac{2\theta^2}{\ln(1.12\theta + 1.3)}\right]\right\}^{-1}. \tag{5}$$

For the electron-electron pair production rate we adopt the expression used by White & Lightman (1989):

$$(\dot{n}_+)_{ee} = c r_e^2 n_e^2 \begin{cases} 2 \times 10^{-4}\theta^{3/2}\exp(-2/\theta)(1 + 0.015\theta), & \text{if } \theta \ll 1, \\ (112/27\pi)\alpha_f^2(\ln\theta)^3(1 + 0.058/\theta)^{-1}, & \text{if } \theta \gg 1, \end{cases} \tag{6}$$

where α_f is the fine structure constant. Local equilibrium requires that $(\dot{n}_+)_{ee} = (\dot{n}_+)_{\rm ann}$, which allows us to solve for z as a function of the plasma temperature. We find that for the highest temperature of interest, $T = 10^{11}$ K, z has a maximum value ~ 0.1, and that it decreases monotonically in cooler plasmas. This implies that our low-z assumption is self-consistent.

Given z, we can compute the total number density of electrons in the disk, $n_e = n_p(1 + z)$, and the number density of electrons plus positrons, $n_\pm = n_p(1 + 2z)$.

2.3. *Cooling Processes*

Since ions are considerably more massive than electrons and positrons, viscous heating will affect primarily the ions (SLE; Phinney 1981; Rees et al. 1982), which will then transfer this energy to the electrons. In their paper, NY assume that the energy transfer occurs only by way of Coulomb interactions; they ignore possible nonthermal coupling mechanisms (e.g., Begelman

& Chiueh 1988). Since Coulomb interactions are not efficient at low densities, the ions are always hotter than the electrons. In this paper, we assume that the ions and electrons have been brought into thermal equilibrium by some process, without explicitly specifying the actual coupling mechanism.

The cooling of the hot plasma occurs mainly through the electrons and positrons. In our model, we consider three cooling processes: bremsstrahlung, synchrotron, and Compton cooling by both bremsstrahlung and synchrotron photons.

2.3.1. *Bremsstrahlung Cooling*

The free-free radiation in a plasma is produced through five different types of interactions: electron-electron (e^-e^-), electron-ion (e^-i), positron-electron (e^-e^+), positron-positron (e^+e^+), and positron-ion (e^+i). However, e^-i and e^+i processes can be combined together since their corresponding cooling rates are identical, and the same is true for e^-e^- and e^+e^+ processes. Thus, the total bremsstrahlung cooling rate per unit volume is just the sum of the rates for $e^\pm i$, $e^\pm e^\pm$, and e^-e^+ processes; and we can write $q_{\rm br}^- = q_{ei}^- + q_{ee}^- + q_{+-}^-$, provided we replace $n_p n_e$ by $n_p n_\pm$ and n_e^2 by $(n_e^2 + n_+^2)$ in our calculations of q_{ei}^- and q_{ee}^-, respectively.

Following NY, we adopt these expressions from Stepney & Guilbert (1983) and Svensson (1982) for the $e^\pm i$, $e^\pm e^\pm$, and e^-e^+ bremsstrahlung cooling rates:

$$q_{ei}^- = 1.48 \times 10^{-22} n_p n_\pm F_{ei} \text{ ergs cm}^{-3} \text{ s}^{-1} ; \tag{7}$$

$$q_{ee}^- = \begin{cases} 2.56 \times 10^{-22}(n_e^2 + n_+^2)\theta^{1.5}(1 + 1.1\theta + \theta^2 - 1.25\theta^{2.5}) \text{ ergs cm}^{-3} \text{ s}^{-1} , & \text{if } \theta < 1 ; \\ 3.42 \times 10^{-22}(n_e^2 + n_+^2)\theta[\ln(1.123\theta) + 1.28] \text{ ergs cm}^{-3} \text{ s}^{-1} , & \text{if } \theta \geq 1 , \end{cases} \tag{8}$$

$$q_{+-}^- = \begin{cases} 3.43 \times 10^{-22} n_e n_+ (\theta^{0.5} + 1.7\theta^2) \text{ ergs cm}^{-3} \text{ s}^{-1} , & \text{if } \theta < 1 , \\ 6.84 \times 10^{-22} n_e n_+ \theta[\ln(1.123\theta) + 1.24] \text{ ergs cm}^{-3} \text{ s}^{-1} ; & \text{if } \theta \geq 1 , \end{cases} \tag{9}$$

where

$$F_{ei} = \begin{cases} 4\sqrt{\dfrac{2\theta}{\pi^3}}(1 + 1.781\theta^{1.34}) , & \text{if } \theta < 1 , \\ \dfrac{9\theta}{2\pi}[\ln(1.123\theta + 0.48) + 1.5] , & \text{if } \theta \geq 1 , \end{cases} \tag{10}$$

2.3.2. *Synchrotron Cooling*

Synchrotron cooling is very important in our model, both because we assume an equipartition magnetic field in the disk and because we consider relativistic temperatures for the electrons and positrons.

Pacholczyk (1970) has calculated the spectrum of synchrotron emission by a relativistic Maxwellian distribution to be

$$\epsilon_s \, dv = 4.43 \times 10^{-30} \frac{4\pi\nu n_\pm}{K_2(1/\theta)} I\left(\frac{x_M}{\sin\phi}\right) dv \text{ ergs cm}^{-3} \text{ s}^{-1} , \tag{11}$$

where

$$x_M = \frac{2\nu}{3\nu_0 \theta^2} , \qquad \nu_0 = \frac{eB}{2\pi m_e c} ,$$

ϕ is the angle between the velocity vector of the electrons and the direction of the local magnetic field, and $I(x)$ is a tabulated function. Positrons produce synchrotron radiation at the same rate as electrons do, and, therefore, in equation (11) we have used the total number density, $n_\pm$, instead of n_e.

For an isotropic velocity distribution we can average $I(x_M/\sin\phi)$ over ϕ to get a new function $I'(x_M)$, for which the following fitting function was found by Mahadevan, Narayan, & Yi (1996):

$$I'(x_M) = \frac{4.0505}{x_M^{1/6}}\left(1 + \frac{0.40}{x_M^{1/4}} + \frac{0.5316}{x_M^{1/2}}\right) \exp(-1.8899 x_M^{1/3}) . \tag{12}$$

We substitute this function for $I(x_M/\sin\phi)$ in equation (11).

Equations (11) and (12) are valid only for optically thin emission. However, below some critical frequency ν_c the emission becomes self-absorbed, and that has to be taken into account in computing the total cooling rate. We estimate ν_c as the frequency at which the synchrotron emission from a thin annulus of height $2H$, radius R, and thickness ΔR is equal to the blackbody emission (in the Rayleigh-Jeans limit) from the upper and lower surfaces of the annulus (NY presented a similar argument, but they used a spherical rather than cylindrical geometry). This condition gives us the equation

$$2H(2\pi R \, \Delta R)\epsilon_s \, dv = 2(2\pi R \, \Delta R) 2\pi \frac{\nu_c^2}{c^2} kT \, dv , \tag{13}$$

which we can solve numerically for given values of R, H, and T to obtain ν_c.

Given the value of the critical frequency, we can estimate the total synchrotron emission per unit volume as follows. We assume that for frequencies below ν_c the emission is completely self-absorbed, so that the volume emissivity can be approx-

imated by the blackbody emission from the surface of the disk divided by the disk volume. Above ν_c the emission is optically thin and equation (11) can be used. To get the total cooling per unit volume by synchrotron emission, we then integrate over frequency:

$$q_s^- = \frac{2\pi R^2}{2H\pi R^2}\int_0^{\nu_c} 2\pi\frac{\nu^2}{c^2}kT\,d\nu + \int_{\nu_c}^{\infty}\epsilon_\nu\,d\nu$$
$$= \frac{2\pi kT\nu_c^3}{3Hc^2} + (6.76\times 10^{-28})\frac{n_\pm}{K_2(1/\theta)a_1^{1/6}}$$
$$\times\left[\frac{1}{a_4^{11/2}}\Gamma\left(\frac{11}{2}, a_4\nu_c^{1/3}\right) + \frac{a_2}{a_4^{19/4}}\Gamma\left(\frac{19}{4}, a_4\nu_c^{1/3}\right) + \frac{a_3}{a_4^4}(a_4^3\nu_c + 3a_4^2\nu_c^{2/3} + 6a_4\nu_c^{1/3} + 6)e^{-a_4\nu_c^{1/3}}\right], \quad (14)$$

where the parameters a_1, a_2, a_3, and a_4 are defined as

$$a_1 = \frac{2}{3\nu_0\theta^2}, \qquad a_2 = \frac{0.4}{a_1^{1/4}}, \qquad a_3 = \frac{0.5316}{a_1^{1/2}}, \qquad a_4 = 1.8899a_1^{1/3}, \quad (15)$$

and $\Gamma(a, x) = \int_x^\infty t^{a-1}e^{-t}\,dt$.

2.3.3. *Compton Cooling*

Since our solutions are hot, Comptonization of soft photons by hot electrons becomes an important cooling mechanism. It is an especially important process for higher values of the accretion rate when the scattering depth is of order unity and synchrotron emission is the dominant photon production mechanism, i.e., most photons are initially very soft.

We compute the Compton cooling rate using the Comptonized energy enhancement factor η, which is defined as the average ratio of the energy of a photon at escape to its initial energy. We adopt the following prescription for η, which is derived in Appendix A:

$$\eta = e^{s(A-1)}[1 - P(j_m + 1, As)] + \eta_{\max}P(j_m + 1, s), \quad (16)$$

where $P(a, x) = [1/\Gamma(a)]\int_0^x t^{a-1}e^{-t}\,dt$ is the incomplete gamma function and

$$A = 1 + 4\theta + 16\theta^2, \qquad s = \tau_{es} + \tau_{es}^2,$$
$$j_m = \ln(\eta_{\max})/\ln(A), \qquad \eta_{\max} = \frac{3kT}{h\nu}. \quad (17)$$

The parameter A is the average increase in energy of a soft photon in each scattering by a Maxwellian distribution of electrons (and positrons) at temperature θ, $\tau_{es} = 2n_\pm\sigma_T H$ is the Thomson optical depth (counting both electrons and positrons), j_m is the number of scatterings required for the maximum possible energy enhancement $\eta_{\max}$, and ν is the initial photon frequency. By definition, the Comptonized flux is the original flux multiplied by η.

Since the synchrotron spectrum is strongly peaked at the critical frequency ν_c, we estimate the cooling rate caused by the Comptonization of the synchrotron radiation simply by computing η for $\nu = \nu_c$:

$$q_{C,s}^- = \eta(\nu_c)q_s^-. \quad (18)$$

The spectrum of bremsstrahlung radiation is practically flat for frequencies between the bremsstrahlung self-absorption frequency, ν_{br}, and the exponential cutoff at $\nu = kT/h$. The emission at frequencies $\nu < \nu_{br}$ is negligible compared with the integrated bremsstrahlung cooling rate. Therefore, we can approximate free-free emission per unit frequency as the ratio $q_{br}^-/[(kT/h) - \nu_{br}]$. We estimate ν_{br} as the frequency at which the free-free absorption opacity, κ_ν^{ff} (which is frequency dependent) is equal to the electron scattering opacity, κ_{es}. Below ν_{br} Comptonization is not important, because absorption dominates over scattering. Therefore, to calculate the Comptonization enhancement we perform the following numerical integration:

$$q_{C,br}^- = \int_{\nu_{br}}^{kT/h}\eta(\nu)\frac{dq_{br}^-}{d\nu}\,d\nu = \int_{\nu_{br}}^{kT/h}\eta(\nu)\frac{q_{br}^-}{(kT/h) - \nu_{br}}\,d\nu. \quad (19)$$

2.3.4. *Cooling of the Optically Thick Gas*

The total cooling rate for the optically thin gas is simply the sum of the two components calculated above:

$$q^- = q_{C,br}^- + q_{C,s}^-. \quad (20)$$

This rate is appropriate for the hot solutions, which are generally optically thin. However, to reproduce the equilibrium solution corresponding to the cool optically thick Shakura & Sunyaev disk, we use the following generalized cooling formula given by NY:

$$q^- = \frac{4\sigma T^4/H}{1.5\tau + \sqrt{3} + (4\sigma T^4/H)(q_{C,br}^- + q_{C,s}^-)^{-1}}, \quad (21)$$

where $\tau = \tau_{es} + \tau_{abs}$ is the total optical depth of the disk in the vertical direction and $\tau_{abs} = (H/4\sigma_B T^4)(q^-_{C,br} + q^-_{C,s})$ is the optical depth for absorption. For a small optical depth, equation (21) reduces to equation (20), and therefore this formula can be used in the limit of both very high and very low optical depth.

2.3.5. *Radiation Pressure*

The total cooling rate allows us to compute the radiation pressure in the disk:

$$p_r = \frac{q^- H}{2c}\left(\tau + \frac{2}{\sqrt{3}}\right). \tag{22}$$

The gas pressure in the accreting flow is simply

$$p_g = \rho k T\left(\frac{1}{\mu_i m_u} + \frac{1}{\mu_e m_u}\right), \tag{23}$$

where μ_i and μ_e are the effective molecular weights of the ions and electrons, given by

$$\mu_i = \frac{4}{1+3X} = 1.23\,, \qquad \mu_e = \frac{2}{1+X} = 1.14\,, \tag{24}$$

with numerical values computed for a hydrogen mass fraction $X = 0.75$ (NY). Given p_r and p_g, the parameter χ, defined in § 2.1, is readily computed as

$$\chi = \beta/\beta_m = p_g/(p_r + p_g)\,. \tag{25}$$

3. PROPERTIES OF THE SOLUTIONS

An equilibrium thermal state for the accretion flow requires that viscous heating minus the advected energy is exactly balanced by the total radiative cooling at each radius:

$$q^+(1-f) = q^-\,. \tag{26}$$

For fixed values of m, r, $\dot{m}$, and β_m, the equations (1)–(26) comprise a closed set, which can be solved to obtain all the relevant parameters of the accretion flow. We solve the equations numerically using T and χ as free variables. We begin by assuming arbitrary values for T and χ, and we use equations (2)–(6) to calculate all the parameters of the plasma, including the pair fraction. Then we use equations (7)–(24) to calculate the cooling rate q^- and the gas and radiation pressures, p_g and p_r. Now we compute $\chi = p_g/(p_r + p_g)$ (see eq. [25]) and compare the result with the initially assumed value. If the two values are not equal, we vary χ keeping T fixed until there is agreement between the initial and final χ. We then vary T, optimizing χ at each step, until the energy equation (26) is satisfied. At this point, we have a self-consistent equilibrium solution.

All calculations presented below were done for an equipartition magnetic field strength in the disk, $\beta_m = 0.5$. However, we have found that models with $\beta_m = 0.95$ (where magnetic pressure constitutes only 5% of the total pressure) produce practically the same results.

Figure 1 illustrates the variations with T of the two sides of equation (26); the solid line shows $q^+(1-f)$ and the dashed line shows the total radiative cooling q^-. These results are for a single-temperature accretion disk of mass accretion rate $\dot{M} = 10^{-5}\dot{M}_{Edd}$, around a black hole of mass $M = 10\,M_\odot$, and at a radial distance $R = 10R_{Schw}$; χ has been optimized at each T. The three points at which the two curves intersect, labeled as 1, 2, and 3 on the figure, correspond to three equilibrium states of the accretion disk wherein the energy balance equation (26) is satisfied. The equilibrium point 1 corresponds to the standard Shakura & Sunyaev (1973) thin disk; the middle point is the one-temperature equivalent of the unstable Shapiro et al. (1976) solution; the equilibrium point labeled 3 is a new hot solution that does not seem to have been discussed before in the literature. It is related to the advection-dominated one-temperature solution of Abramowicz et al. (1995), but with some important differences as we argue later.

Note that the slope of the cooling curve in Figure 1 changes twice. At $T \approx 10^{6.2}$ K the change of slope indicates a transition from an optically thick to an optically thin flow. There is a corresponding kink in the heating curve, since at this point the cooling rate is at its maximum and radiation pressure briefly dominates over the gas pressure, causing a sharp decrease in gas density. For $T < 10^{6.2}$ K, the gas cools as a blackbody and the cooling rate increases with increasing temperature. For $T > 10^{6.2}$ K, the dominant cooling process is optically thin bremsstrahlung, which is less efficient at higher temperatures. At $T \approx 10^{9.5}$ K the slope of log (q^-) changes again, indicating a point at which synchrotron radiation becomes the dominant cooling process. In contrast to bremsstrahlung, the synchrotron emission increases with increasing temperature, hence the positive slope of the cooling curve at these high temperatures.

By inspection, it is clear that equilibria 1 and 3 are thermally stable. In both of these equilibria, if the gas is perturbed to a higher temperature, the rate of cooling becomes greater than the rate of heating, allowing the medium to cool back to the equilibrium value of T. Similarly, if T becomes slightly smaller, the heating rate exceeds the cooling rate and the gas heats up back to the equilibrium temperature. Equilibrium 2, on the other hand, is unstable. Here a small increase or decrease in T leads to a runaway situation in which T deviates progressively more rapidly from the equilibrium value.

We have computed the properties of the accreting gas corresponding to the three equilibria for different values of $\dot{M}$. The resulting curves for a central black hole of mass $M = 10\,M_\odot$ at fixed radial distance $R = 10R_{Schw}$ are plotted in Figure 2 for

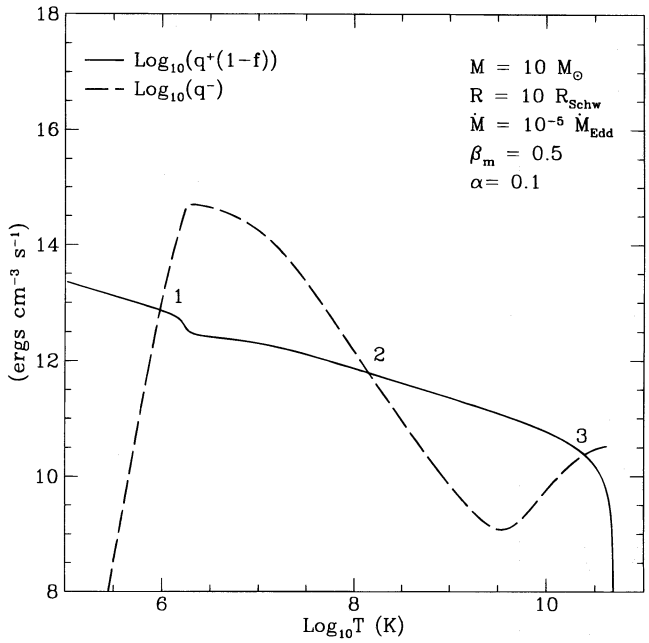

FIG. 1.—Rates of heating (*solid line*) and cooling (*dashed line*) of the accreting single-temperature gas plotted vs. gas temperature, T. Intersection points of the two curves mark equilibrium states of the system. Point 1 corresponds to the standard thin disk solution, point 2 is equivalent to the unstable SLE solution, and point 3 is our new, hot, thermally and viscously stable solution.

$\alpha = 0.1$ (*heavy line*) and $\alpha = 1.0$ (*thin line*). The curves are labeled 1, 2, and 3 to indicate correspondence with the equilibria labeled 1, 2, 3 in Figure 1. The six panels in Figure 2 show how various physical properties of the solutions depend on the accretion rate. The unstable SLE solution (branch 2) is indicated by a dashed line.

For $\alpha = 0.1$, the topology of our results is qualitatively similar to that of the corresponding solutions for two-temperature disks described by Chen et al. (1995). We see that the two hotter branches merge together at some critical accretion rate $\dot{M}_{\rm crit}$, above which the cooling in the disk is so efficient that the only equilibrium allowed is the standard thin disk solution. For $\alpha = 1$, the hot branch extends to much higher values of the accretion rate; in fact, the value of $\dot{M}_{\rm crit}$ goes up by ~ 2 orders of magnitude, in agreement with the results of Abramowicz et al. (1995) and NY. Somewhat surprisingly, the topology of the solution curves for $\alpha = 1$ continues to be similar to that for $\alpha = 0.1$. This is different from the result reported by Chen et al. (1995), who found that for $\alpha = 1$ the middle branch merged with the cold disk solution, whereas the hottest branch extended independently upward to become the optically thick advection-dominated solution, discovered by Abramowicz et al. (1988). The value of the critical α, at which the topology changes, is, however, sensitive to the details of the radiation processes included in the model (M. Abramowicz, 1995 private communication). In fact, we find the same topology change in our results when we push α above ~ 1.7.

For both $\alpha = 0.1$ and $\alpha = 1$, the curves corresponding to the three equilibria in Figure 2*a* have positive slopes, i.e., $\partial \dot{M}/\partial \Sigma > 0$. This implies that all three solutions are viscously stable (cf. Frank et al. 1992, p.103). Note also that our new hot solution is optically thin for all values of $\dot{M}$ where the solution exists (Fig. 2*b*) and cools mainly through synchrotron and Comptonized synchrotron processes (Fig. 2*c*).

Figure 3 directly compares the two-temperature (*thin line*) and one-temperature (*heavy line*) equilibrium solutions for a disk with $\alpha = 0.1$. For temperatures below $T \approx 10^9$ K, the two curves merge because the electron and ion temperatures in the two-temperature solution are nearly equal (Fig. 3*c*); therefore, two-temperature and one-temperature solutions are effectively the same. However, for $T \gtrsim 10^9$ K, the two solutions differ significantly. The most important distinction is in the value of the advected energy fraction f (Fig. 3*c*). For the hot two-temperature solution, we have $f \rightarrow 1$ at all $\dot{M}$, showing that this branch is always advection-dominated. In contrast, we see that our one-temperature hot solution is cooling dominated ($f < 0.1$) for a wide range of accretion rates. This is a completely new result; prior to this the only hot stable solutions known were all advection-dominated (NY; Abramowicz et al. 1995; Chen 1995; Chen et al. 1995). Since the cooling rate is given by $q^- = q^+(1 - f)$, we see that, at a given accretion rate, our single-temperature disk with its low value of f is considerably more luminous than the equivalent two-temperature flow.

In the case of the two-temperature advection-dominated hot solutions discussed by NY and Abramowicz et al. (1995), the thermal stability of the solution to long-wavelength perturbations has been shown to be the direct result of advection. However, our hot one-temperature solution branch 3 is cooling dominated and has very little advection. Why is this solution stable? The answer is obvious from Figure 1, where we see that the introduction of synchrotron cooling causes the cooling curve $q^-(T)$ to be steeply positive for $T > 10^{9.5}$ K. Therefore, thermal stability is achieved in this solution because of the usual reason, namely that the cooling increases more rapidly than the heating. Note that we would not have obtained this result if we had included only bremsstrahlung cooling. In fact, Abramowicz et al. (1995) considered the pure bremsstrahlung one-temperature case, and they obtained a hot advection-dominated solution. Thus, the inclusion of synchrotron cooling has an

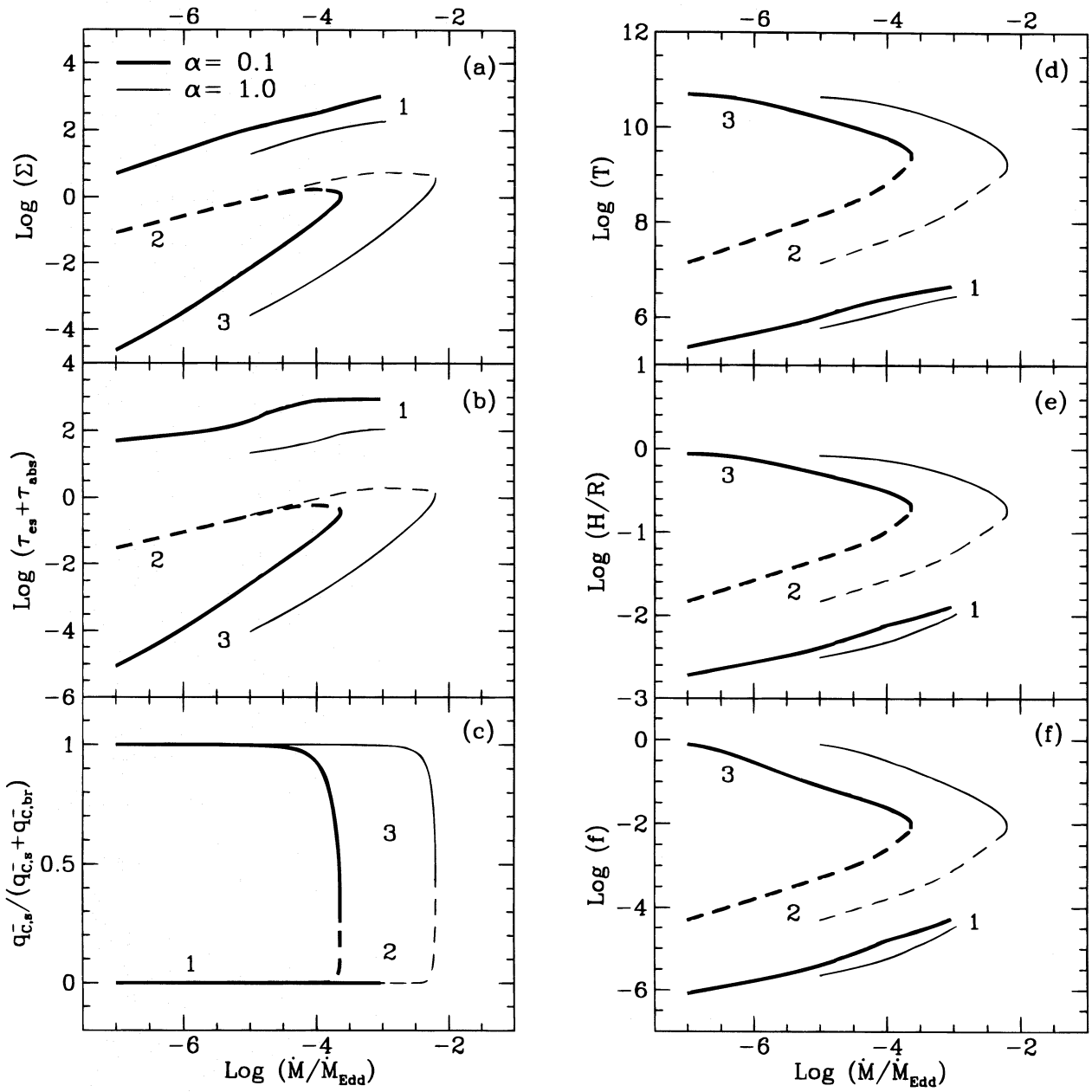

FIG. 2.—Thermal equilibria of single-temperature accretion disks with $\beta_m = 0.5$ around a 10 $M_\odot$ black hole at a radius of $R = 10R_{Schw}$. Heavy and thin lines represent solutions with $\alpha = 1$ and $\alpha = 0.1$, respectively. The three branches, labeled 1, 2, and 3, correspond to the standard thin disk, unstable SLE disk (indicated by a dashed line), and our hot and stable solution (as in Fig. 1), respectively. In the six panels, we plot (*a*) surface density, Σ (g cm^{-2}), (*b*) total optical depth, ($\tau_{es} + \tau_{abs}$), (*c*) fraction of the total cooling due to Comptonized synchrotron radiation, (*d*) temperature, T (K), (*e*) the vertical scale height, H/R, and (*f*) advected energy fraction, f; all are plotted as functions of the accretion rate $\dot{M}$. Note that the hot solution branch (labeled 3) is optically thin, has essentially spherical geometry ($H/R \approx 1$), and cools mainly by synchrotron radiation.

important effect on the basic physics of the accretion flow. Although a full linear stability analysis along the lines of Kato et al. (1996) has not been done on our new solutions, we suspect that these solutions are stable to all linear perturbations, regardless of wavelength.

Figure 4 illustrates the radial structure of a disk, with $\alpha = 0.1$, for a fixed value of the accretion rate, $\dot{M} = 10^{-4}\dot{M}_{Edd}$. The inner edge was chosen to be at $R = 3R_{Schw}$, corresponding to the last stable orbit. As expected, we see that the two-temperature (*thin line*) and one-temperature (*heavy line*) solutions merge at large radii at which the temperature is low and even the two-temperature plasma has effectively a single temperature (see Fig. 4*c*). Thus, away from the center, the flow is advection-dominated (see Fig. 4*b*) and almost spherical with $H/R \sim 1$ (Fig. 4*d*), regardless of whether we have a two-temperature or one-temperature solution. However, closer to the accreting object, the flow becomes increasingly cooling dominated in the one-temperature case and settles into a disk with $H/R \sim 0.15$ at the inner edge. The resulting geometry—fairly thin disk near the inner edge and quasi-spherical flow at larger radii—is unusual for accretion disk models. Another interesting feature of our one-temperature solution is that the temperature profile of the disk is not monotonic but has a

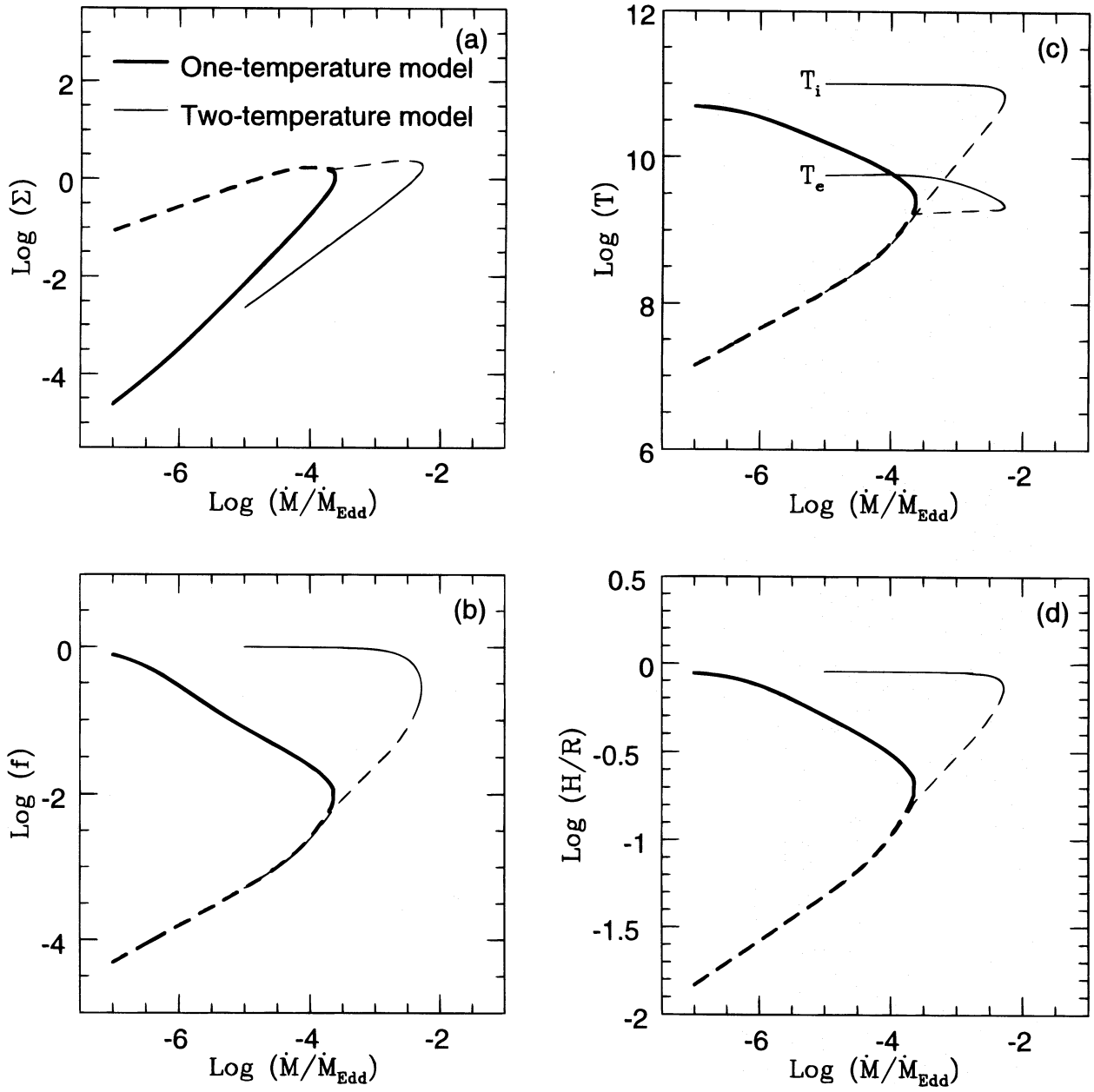

FIG. 3.—Thermal equilibria of single-temperature (*heavy line*) and two-temperature (*thin line*) accretion disks, with $\beta_m = 0.5$ and $\alpha = 0.1$, around a $10\,M_\odot$ black hole at a radius of $r = 10$. The thin disk branch is not shown. The four panels show (*a*) surface density, Σ (g cm^{-2}), (*b*) advection parameter, f, (*c*) temperature, T (K), and (*d*) the scale height, H/R, plotted as functions of $\dot{M}$. The unstable branch is shown by dashed lines. On the stable branch, the single-temperature solution is less advection dominated and has a higher electron temperature than the two-temperature solution.

well-defined maximum at $R \sim 40R_{\rm Schw}$. Therefore, the hottest part of the spectrum does not come from the inner edge of the disk.

NY showed that their advection-dominated hot two-temperature solution exists only for accretion rates $\dot{M}$ less than a critical rate $\dot{M}_{\rm crit}$, which depends on α and R (see also Abramowicz et al. 1995). We find a similar result also in the case of our cooling-dominated hot one-temperature solution. Figure 5 shows the critical accretion rate $\dot{M}_{\rm crit}$ for our solution as a function of R, as well as the variation of the gas temperature. The two panels on the left (Figs. 5*a* and 5*b*) compare the results for the one-temperature and two-temperature solutions for $\alpha = 0.1$. We see that the electron temperatures for the two solutions are nearly equal, but the behavior of $\dot{M}_{\rm crit}$ is quite different in the two cases. For a two-temperature flow, $\dot{M}_{\rm crit}$ is roughly independent of R for $R \lesssim 10^3 R_{\rm Schw}$ and is given approximately by $\dot{M} \sim 0.3\alpha^2 \dot{M}_{\rm Edd}$ (see, for a discussion of the α^2 scaling, NY and Abramowicz et al. 1995). In contrast, $\dot{M}_{\rm crit}$ decreases almost linearly with decreasing R in the one-temperature case, so that $\dot{M} \sim 3 \times 10^{-3}\alpha^2 (R/R_{\rm Schw})\dot{M}_{\rm Edd}$ for $R \lesssim 10^3 R_{\rm Schw}$. Thus, near the black hole, $\dot{M}_{\rm crit}$ for the one-temperature solution is smaller than that of the two-temperature solution by as much as 2 orders of magnitude.

The steep decrease of $\dot{M}_{\rm crit}$ with decreasing R leads to an interesting effect that is already seen in Figure 4. For a wide range of $\dot{M}$, it is possible to have $\dot{M} < \dot{M}_{\rm crit}$ at large radii, but to have $\dot{M} > \dot{M}_{\rm crit}$ at small radii, with a transition at some critical

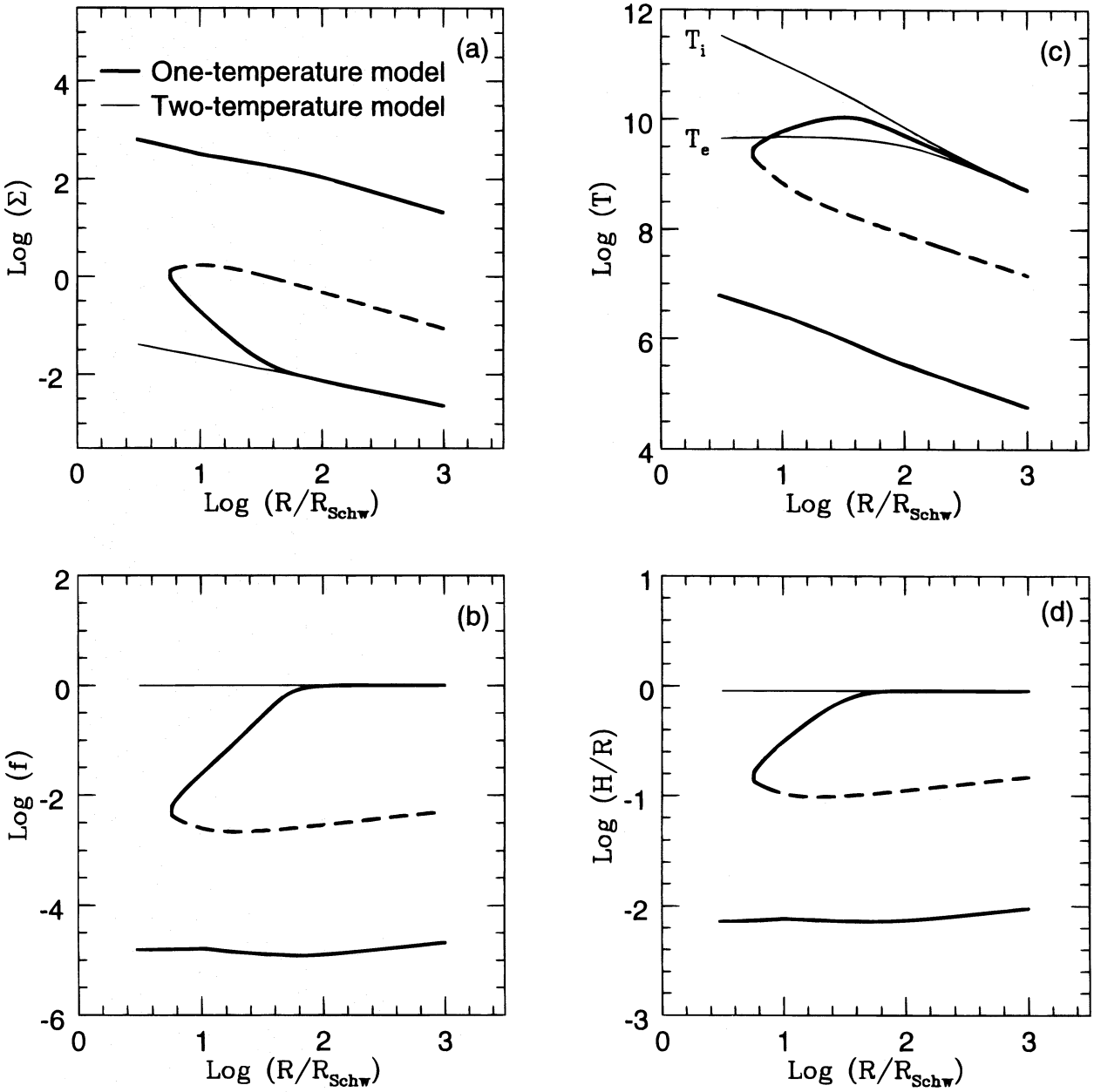

FIG. 4.—Radial profiles of thermal equilibria for a single-temperature accretion disk, with $\beta_m = 0.5$, $\alpha = 0.1$, and $\dot{M}/\dot{M}_{\rm Edd} = 10^{-4}$, around a $10\,M_\odot$ black hole (*heavy line*). For comparison, we also plot the hot stable branch of the two-temperature disk (*thin line*). As expected, the two models give identical results at large radii. Closer to the black hole, however, the single-temperature solution becomes cooling-dominated, while the two-temperature solution remains advection-dominated. Note the maximum in the disk temperature at $R \approx 40R_{\rm Schw}$.

radius $R_{\rm min}$. For the example shown in Figure 4, we have $R_{\rm min} = 5R_{\rm Schw}$. In this case, we can have a hot one-temperature solution for $R > R_{\rm min}$, but the solution disappears at $R = R_{\rm min}$. Below $R_{\rm min}$, the only equilibrium solution available is the cool thin accretion disk. (Note that, because of the very low $\dot{M} \sim 10^{-4}\dot{M}_{\rm Edd}$, the Lightman-Eardley instability does not affect the thin disk solution in this case.) Thus, the example shown in Figure 4 has an extremely unusual structure. For $3R_{\rm Schw} < R < 5R_{\rm Schw}$, there is a standard thin disk. Then for $5R_{\rm Schw} < R < 40R_{\rm Schw}$, we have a hot, but cooling-dominated, fairly thick disk. Finally, for $R > 40R_{\rm Schw}$, we have a regular advection-dominated quasi-spherical flow. There are several discussions in the literature of models in which an outer thin disk makes a transition to a hot inner flow (e.g., SLE; Wandel & Liang 1991; Narayan et al. 1996a; Narayan 1996), but here we have an example of a model that does the opposite; it transforms from an outer hot advection-dominated flow through a cooling-dominated hot flow to an inner thin disk. (See Melia 1994 for the closest example discussed previously in the literature.)

Figure 6 shows how the properties of the flow change as the accretion rate is reduced. There are some interesting effects. First, with decreasing $\dot{M}$, the critical radius $R_{\rm min}$ disappears so that there is no longer any reason for the gas to make a transition to a cool disk on the inside. As $\dot{M}$ decreases still further, even the cooling-dominated zone of the hot disk disappears and advection becomes more important throughout the flow. Consequently, the disk thickens considerably, and the

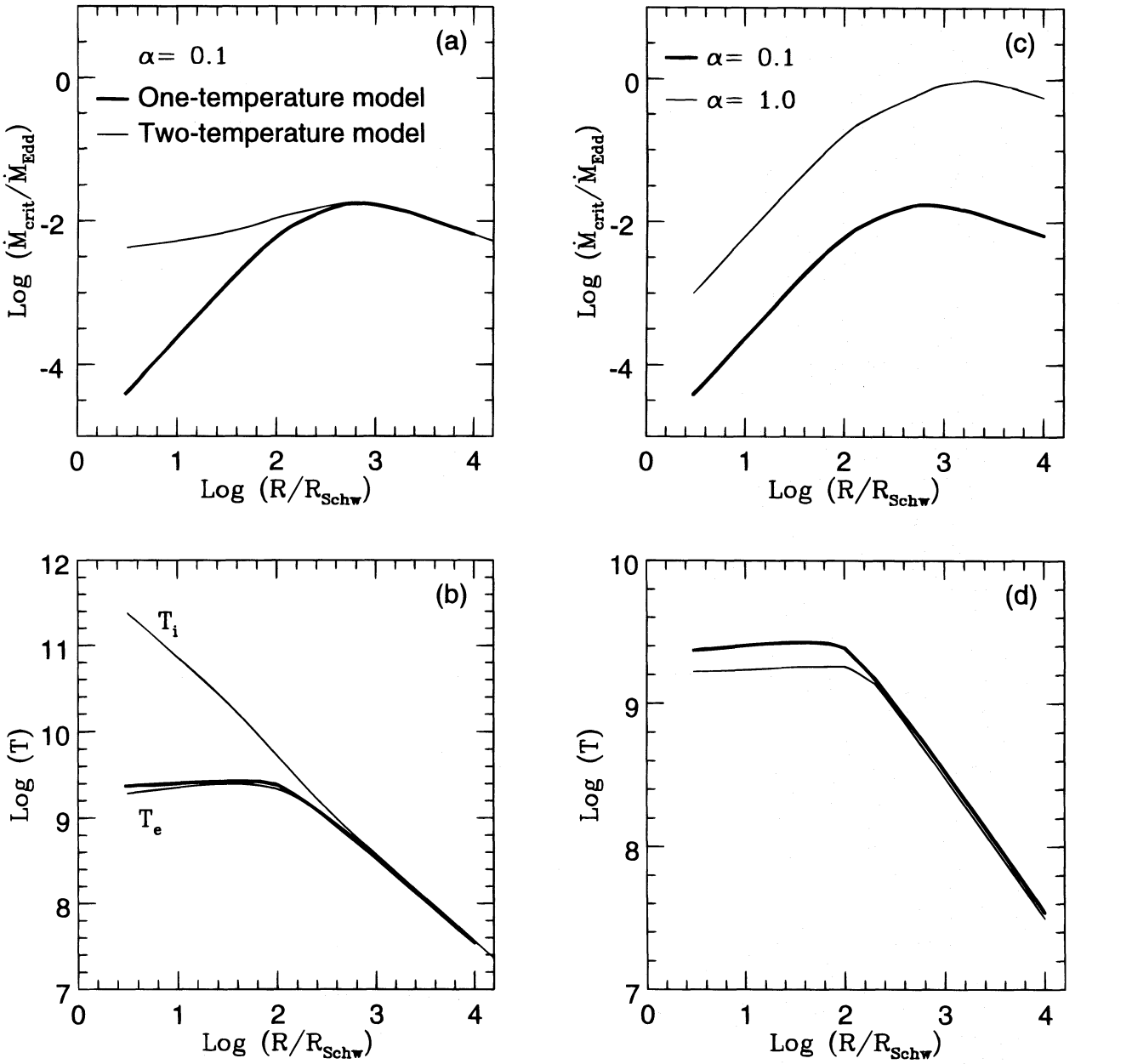

FIG. 5.—Critical accretion rate $\dot{M}_{\rm crit}$ (*upper panels*) and corresponding temperature (*lower panels*) are plotted as functions of the radius. Panels (*a*) and (*b*) compare the results for the one- and two-temperature models for $\beta_m = 0.5$ and $\alpha = 0.1$. The critical $\dot{M}$ differs significantly in the two models, but the gas temperature in the single-temperature model is almost always equal to T_e in the two-temperature model. Panels (*c*) and (*d*) show the results for a single-temperature disk with $\beta_m = 0.5$ and two different values of α. Note that, although $\alpha = 1.0$ allows models with values of $\dot{M}_{\rm crit}$ higher by 2 orders of magnitude, the corresponding temperatures do not depend strongly on α.

maximum in the temperature profile at large radius becomes less apparent. For $\alpha = 0.1$ and $\dot{M}/\dot{M}_{\rm Edd} < 10^{-8}$, the flow is advection dominated and nearly virial at all radii.

Figure 6*c* shows the relative importance of Comptonized synchrotron cooling as a function of R at various $\dot{M}$. We see that synchrotron and Comptonized synchrotron cooling is dominant in the inner regions, $R < 100R_{\rm Schw}$, regardless of the accretion rate. In the outer disk, on the other hand, where the flow is cooler and more advection dominated, the cooling is mostly due to bremsstrahlung emission.

Though one-temperature solutions are restricted to smaller values of $\dot{M}$ than the corresponding two-temperature solutions, nevertheless, we should note that for any given $\dot{M}$ they are significantly more luminous. This is because these flows are cooling-dominated at small radii, where most of the energy is dissipated. Figure 7*a* illustrates this luminosity increase in the case of $\alpha = 0.3$. Here we plot the total disk luminosity as a function of $\dot{M}$ for one-temperature (*solid line*) and two-temperature (*dashed line*) solutions. Note that at $\dot{M} = 10^{-4}\dot{M}_{\rm Edd}$, the one-temperature disk is $\sim 10^4$ times more luminous than its two-temperature counterpart.

Figure 7*b* shows how the total luminosity of our one-temperature solutions changes with α. For a given value of $\dot{M}$, higher α solutions are less luminous because they are more advection dominated (see Fig. 2*e*). However, higher values of α allow the

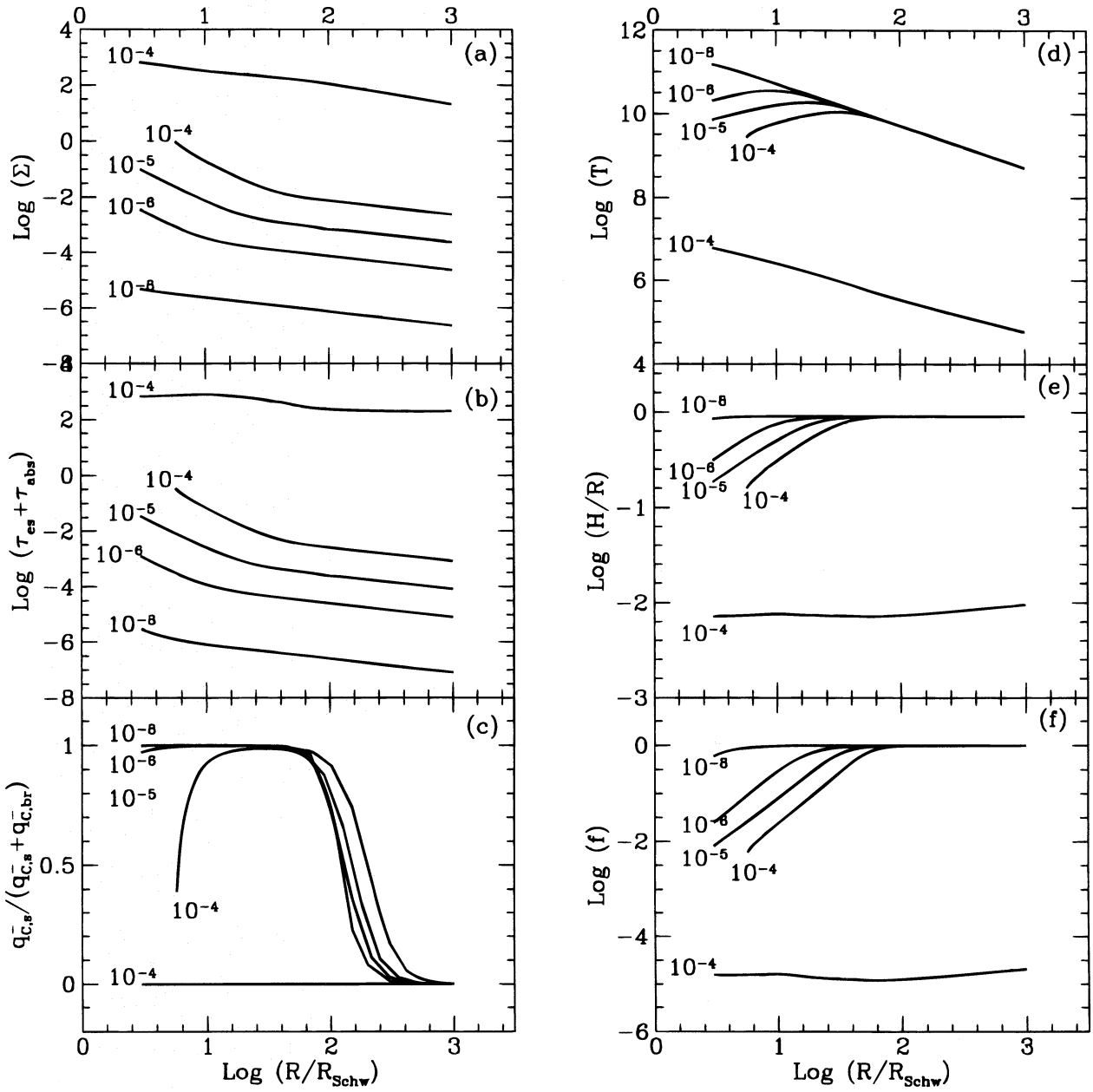

FIG. 6.—Radial profiles of hot single-temperature solutions, labeled by the values of the accretion rate in units of $\dot{M}_{Edd}$. The other parameters have the same values as in Fig. 4. Note that, for $\dot{M} = 10^{-4}\dot{M}_{Edd}$, the hot branch does not extend all the way to the inner edge of the disk at $R = 3R_{Schw}$. Therefore, the only stable configuration at very small radii is the thin disk solution, which is also shown on the figure.

hot solution to survive up to higher accretion rates (see Fig. 5*c*), with correspondingly higher luminosities. Thus, the most luminous system that we can model as a hot one-temperature disk extending down to $R = 3R_{Schw}$ requires $\alpha = 1.0$ and $\dot{M} = 10^{-3}\dot{M}_{Edd}$, and has a total luminosity $L = 10^{-2.8}L_{Edd}$. We could, in principle, use higher values of $\dot{M}$, but then, as discussed above, we would have to include a cool thin disk at small radii ($R < R_{min}$).

4. DISCUSSION

Most of the work done so far on modeling hot accretion disks has been based on two-temperature flows, where the electrons are much cooler than the ions (SLE; Rees et al. 1982; Melia & Misra 1993; Narayan & Yi 1995b; Narayan et al. 1995, 1996a). However, if there exist mechanisms of energy transfer between ions and electrons that are more efficient than Coulomb scattering (Phinney 1981; Rees et al. 1982; Begelman & Chiueh 1988), the plasma might be well coupled and the ions and electrons may have the same temperature. In this paper, we have investigated how the properties of the hot, stable two-temperature solution described by NY and Chen et al. (1995) are altered if ions and electrons in the accreting plasma are constrained to have the same temperature.

We start from the set of equations developed by NY, adding radiation pressure and particle-particle pair production processes, and improving some of the radiative cooling calculations. We solve these equations for various choices of the viscosity parameter, α, and magnetic pressure parameter, β_m, explicitly setting the ion and electron temperatures equal to each

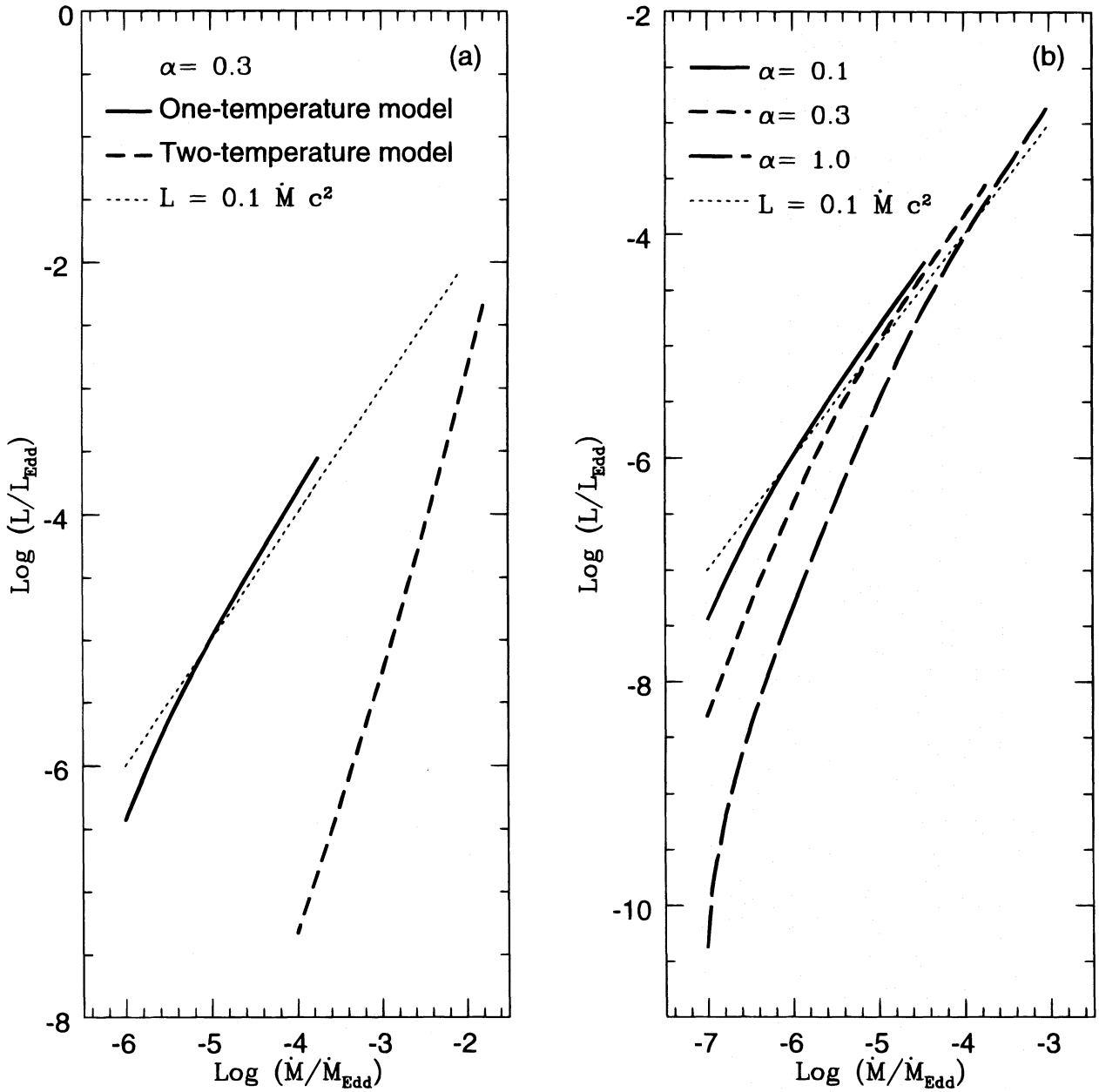

FIG. 7.—(*a*) Compares the integrated luminosities for one- and two-temperature hot accretion disks with $\beta_m = 0.5$, $\alpha = 0.3$, and $M = 10\ M_\odot$. The single-temperature disk is clearly more efficient than a two-temperature disk for a given $\dot{M}$, since its interior regions are cooling dominated. However, the limiting $\dot{M}_{\rm crit}$ of the one-temperature solution is lower than that of the two-temperature flow by 2 orders of magnitude. (*b*) Integrated luminosity of a hot single-temperature accretion disk around a 10 $M_\odot$ black hole, as a function of the mass accretion rate, for $\beta_m = 0.5$ and three different values of α. Each curve was calculated up to the maximum value of the accretion rate given by $\dot{M}_{\rm max} = \dot{M}_{\rm crit}(R = 3R_{\rm Schw})$. The dotted line shows the dependence expected if the radiative efficiency is 10%. Note that disks with lower values of α are more luminous at a given $\dot{M}$, but have a lower limiting accretion rate $\dot{M}_{\rm crit}$.

other. The resulting three branches of solutions that we obtain (Fig. 1) correspond to the standard thin disk (Shakura & Sunyaev 1973; Novikov & Thorne 1973; Lynden-Bell & Pringle 1974), the one-temperature equivalent of the unstable hot solution discovered by SLE, and, finally, a new thermally stable hot solution, whose properties we discuss in detail in § 3. The new solution, which is identified by label 3 in Figures 1 and 2, is the one-temperature equivalent of the two-temperature advection-dominated solutions discussed by NY (see, also, Abramowicz et al. 1995; Chen et al. 1995).

For a viscosity parameter $\alpha = 0.1$, we find that the topological relationships among the three solution branches are similar to those found by Chen et al. (1995) and NY for the two-temperature solutions. Specifically, we see that the two hot branches merge at some maximum value of the mass accretion rate, which we call $\dot{M}_{\rm crit}$, in such a way that for $\dot{M} > \dot{M}_{\rm crit}$ the only solution available to the flow is the standard thin Shakura & Sunyaev disk configuration. At higher α, we confirm the result of Chen et al. (1995) that the topology changes. However, the critical α, where the change occurs, is 1.7 (at $R = 10R_{\rm Schw}$) for the one-temperature case we consider, rather then 0.3, as in Chen et al. (1995).

We have computed the value of the critical mass accretion rate $\dot{M}_{\rm crit}$ as a function of radius for different values of α (Fig. 5*c*) and β_m. We find that $\dot{M}_{\rm crit}$ varies roughly as α^2 (Abramowicz et al. 1995, NY), and it is relatively independent of β_m. A new result is that $\dot{M}_{\rm crit}$ varies almost linearly with R for $R \lesssim R_{\rm Schw}$, since in a two-temperature flow $\dot{M}_{\rm crit}$ is roughly

independent of R in that region. The maximum value of the accretion rate, at which the hot solution exists near the inner disk radius ($R = 3R_{\rm Schw}$), is $\dot{M}_{\rm crit} \sim 3 \times 10^{-3}\alpha^2\dot{M}_{\rm Edd}$. In comparison, two-temperature hot solutions have $\dot{M}_{\rm crit} \sim 0.3\alpha^2\dot{M}_{\rm Edd}$.

Though our single-temperature solutions are limited to lower mass accretion rates than those allowed by two-temperature models, this is compensated to some degree by strong cooling in the inner regions, where $f < 0.5$ for $\dot{M} > 10^{-3}\dot{M}_{\rm crit}(3R_{\rm Schw})$ (Fig. 6*f*). As a result, over the range of mass accretion rates, $10^{-3} < \dot{M}/\dot{M}_{\rm crit}(3R_{\rm Schw}) < 1$, our solutions are significantly more luminous than the corresponding two-temperature solutions (Fig. 7*b*).

This work represents the first example of a hot thermally stable accretion solution that is also cooling-dominated and therefore an efficient radiator. Because advection plays a very minor role in our new solutions, the thermal stability is not the result of advection, as in the equivalent two-temperature solutions (NY, Abramowicz et al. 1995) or in the pure bremsstrahlung one-temperature solutions (Abramowicz et al. 1995). We show that the thermal stability of the hot one-temperature solution is primarily the result of including synchrotron emission, which leads to a rapid increase of the cooling rate with increasing temperature (see Fig. 1).

An interesting feature of our models is the unusual geometry of the flow. Since $\dot{M}_{\rm crit}$ decreases with decreasing R in the inner parts of the disk (see Fig. 5), for a wide range of $\dot{M}$, the disk has a very unusual structure. In the inner regions, where $\dot{M} > \dot{M}_{\rm crit}(R)$, the only possible solution for the accreting gas is the Shakura & Sunyaev thin disk. Note that since we are restricted to relatively low mass accretion rates, the thin disk is viscously stable even at $R \sim 3R_{\rm Schw}$. Further out, the hot solution exists, but it is cooling dominated and therefore has a disklike geometry. Finally, in the outer parts of the disk, the flow is fully advection dominated and becomes nearly quasi-spherical. This interesting result, however, presents a problem for our calculations. The inner radiative zone of the disk is cooler than the outer advection-dominated zone, so the relatively soft photons emitted on the inside will Compton cool the hot outer gas in a way that is incompatible with the local treatment of the radiative processes, which we have used in this paper. The effects of the nonlocal radiation field need to be incorporated self-consistently into future calculations.

Since the gas temperatures in our solutions are on the order of $T \sim 10^{10}$ K, pair production and annihilation processes must be taken into account. In our calculations, we have included particle-particle pair production rates (White & Lightman 1989), which give values for the pair fraction z less than a few percent, but we neglected photon-photon and photon-particle processes. We believe that this treatment is justified for low values of $\dot{m}$ (low optical depth), since bremsstrahlung radiation and Comptonization become unimportant and the cooling is dominated by soft synchrotron photons that are incapable of producing pairs. However, for $\dot{M} \gtrsim 0.1\dot{M}_{\rm crit}$, Comptonization of synchrotron radiation begins to dominate and photon processes may become important. To place a limit on these processes we computed the equilibrium pair density, taking into account photon-photon and photon-particle pair production in the Wien peak of the Comptonized spectrum, using the rates derived by Svensson (1984). The resulting values of z are significantly higher than the values computed taking into account only particle-particle pair production, as $\dot{M}$ approaches $\dot{M}_{\rm crit}$. However, even at $\dot{M} = \dot{M}_{\rm crit}$, the maximum value of z that we find with the inclusion of photon interactions is only about a few percent. Kusunose (1996) and Abramowicz (1996) confirm that pair processes are unimportant in the hot optically thin flows that they have studied. Thus, we believe that our treatment of pair processes is reliable in the entire parameter space we have considered.

This work was supported in part by NSF grant AST 9423209 to the Center for Astrophysics. R. N. thanks the Institute for Theoretical Physics (NSF grant PHY 9407194) for hospitality. I. Y. acknowledges financial support from SUAM Foundation.

APPENDIX A

COMPTONIZATION

Consider a point at an optical depth $\tau_{\rm es}$ inside the medium. The mean number of scatterings of a soft photon escaping from this point is (Rybicki & Lightman 1979)

$$s \approx \tau_{\rm es} + \tau_{\rm es}^2 . \tag{A1}$$

Let the average photon energy change per scattering be A; the initial and final photon energies, $E_{\rm in}$ and $E_{\rm fin}$, are related on average by $E_{\rm fin} = AE_{\rm in}$. For a thermal distribution of electrons with temperature $\theta = kT/(m_e c^2)$, we have (Rybicki & Lightman 1979)

$$A \approx 1 + 4\theta + 16\theta^2 . \tag{A2}$$

The Compton y parameter is simply $y = s(A - 1) = s(4\theta + 16\theta^2)$.

After j scatterings, the energy gain of the photon is A^j, so long as $E_{\rm fin}$ is not saturated to the Wien regime ($E_{\rm fin} \sim 3kT$). The maximum j corresponding to saturation is thus

$$j_m = \ln \eta_{\rm max}/\ln A , \tag{A3}$$

where $\eta_{\rm max} = \eta_{\rm Wien} = 3kT/E_{\rm in}$. The energy enhancement factor, then, is simply the average energy gain of the photon:

$$\eta = \sum_{j=0}^{j_m} A^j P_j + A^{j_m} \sum_{j=j_m+1}^{\infty} P_j , \tag{A4}$$

where P_j is the probability that a photon will suffer exactly j scatterings.

To compute η, we need an expression for P_j. The probability that a photon travels a distance characterized by an optical depth τ_{es} without scattering is $e^{-\tau_{es}}$. To compute P_j, the assumption is usually made that in a medium with $\tau_{es} \lesssim 1$, successive scattering events can be treated independently (e.g., Dermer, Liang, & Canfield 1991), so that P_j can be written as $e^{-\tau_{es}}(1 - e^{-\tau_{es}})^j$. However, for spherical geometry the scattering probability decreases after successive scatterings, because the mean square distance of a photon from the center increases with each scattering. Allowing for this accurately requires Monte Carlo calculations. One limit, however, is straightforward; namely, the case in which the photon continues to travel radially outward after each scattering. In this case, the probability P_j is given by the Poisson formula

$$P_j = \frac{e^{-s}s^j}{j!} . \tag{A5}$$

With the above expression for P_j, we can write η as

$$\eta = e^{-s}\left[\sum_{j=0}^{j_m} \frac{(As)^j}{j!} + A^{j_m} \sum_{j=j_m+1}^{\infty} \frac{s^j}{j!}\right] = e^{-s}\left[e^{As} - \sum_{j=j_m+1}^{\infty} \frac{(As)^j}{j!} + A^{j_m} \sum_{j=j_m+1}^{\infty} \frac{s^j}{j!}\right] . \tag{A6}$$

To evaluate the sums in equation (A6), we define the following function:

$$f(x) = \sum_{j=j_m+1}^{\infty} \frac{x^j}{j!} . \tag{A7}$$

Using integration by parts, and the fact that $f(0) = 0$, it is easy to show that

$$f(x)e^{-x} = \frac{1}{j_m!} \int_0^x e^{-y} y^{j_m} dy \tag{A8}$$

and, therefore,

$$f(x) = \sum_{j=j_m+1}^{\infty} \frac{x^j}{j!} = \frac{e^x}{j_m!} \int_0^x e^{-y} y^{j_m} dy = e^x P(j_m + 1, x) , \tag{A9}$$

where $P(j_m + 1, x)$ is the incomplete gamma function. Substituting this result into equation (A6) yields the final expression for η:

$$\eta = e^{-s}\{[e^{As} - e^{As}P(j_m + 1, As)] + A^{j_m}e^s P(j_m + 1, s)\} = e^{(A-1)s}[1 - P(j_m + 1, As)] + \eta_{\max} P(j_m + 1, s) . \tag{A10}$$

REFERENCES

Abramowicz, M. A. 1996, in Basic Physics of Accretion Disks, ed. S. Kato, S. Inagaki, J. Fukue, & S. Mineshige (New York: Gordon and Breach), in press
Abramowicz, M. A., Chen, X., Kato, S., Lasota, J. P., & Regev, O. 1995, ApJ, 438, L37
Abramowicz, M. A., Czerny, B., Lasota, J. P., & Szuszkiewicz, E. 1988, ApJ, 332, 646
Begelman, M. C., & Chiueh, T. 1988, ApJ, 332, 872
Chen, X. 1995, MNRAS, 275, 641
Chen, X., Abramowicz, M. A., Lasota, J. P., Narayan, R., & Yi, I. 1995, ApJ, 443, L61
Dermer, C. D., Liang, E. P., & Canfield, E. 1991, ApJ, 369, 410
Frank, J., King, A., & Raine, D. 1992, Accretion Power in Astrophysics (Cambridge: Cambridge Univ. Press)
Gilfanov, M., et al. 1995, in NATO ASI Ser., The Lives of the Neutron Stars, ed. M. A. Alpar, U. Kiziloglu, & J. van Paradijs (Dordrecht: Kluwer), vol. 450, 331
Grebenev, S., et al. 1993, A&AS, 97, 281
Harmon, B. A., et al. 1994, in The Second Compton Symp., ed. C. E. Fichtel, N. Gehrels, & J. P. Norris (New York: AIP), 210
Johnson,W. N., et al. 1994, in The Second Compton Symp., ed. C. E. Fichtel, N. Gehrels, & J. P. Norris (New York: AIP), 515
Kato, S., Abramowicz, M. A., & Chen, X. 1996, PASJ, 48, 67
Kinzer, R. L., et al. 1994, in The Second Compton Symp., ed. C. E. Fichtel, N. Gehrels, & J. P. Norris (New York: AIP), 531
Kusunose, M. 1996, in Basic Physics of Accretion Disks, ed. S. Kato, S. Inagaki, J. Fukue, & S. Mineshige (New York: Gordon and Breach), in press
Kusunose, M., & Takahara, F. 1985, Prog. Theor. Phys., 73, 41
———. 1989, PASJ, 41, 263
Lasota, J. P., Abramowicz, M. A., Chen, X., Krolik, J., Narayan, R., & Yi, I. 1996, ApJ, 462, 142
Lightman, A. P., & Eardley, D. M. 1974, ApJ, 187, L1
Luo, C., & Liang, E. P. 1994, MNRAS, 266, 386
Lynden-Bell, D., & Pringle, J. E. 1974, MNRAS, 168, 603
Mahadevan, R, Narayan, R, & Yi, I. 1996, ApJ, in press
Maisack, M., et al. 1993, ApJ, 407, L61
Melia, F. 1994, ApJ, 426, 577
Melia, F., & Misra, R. 1993, ApJ, 411, 797
Narayan, R. 1996, ApJ, 462, 136
Narayan, R., McClintock, J. E., & Yi, I. 1996a, ApJ, 457, 821
Narayan, R., & Yi, I. 1994, ApJ, 428, L13
———. 1995a, ApJ, 444, 231
———. 1995b, ApJ, 452, 710
Narayan, R., Yi, I., & Mahadevan, R. 1995, Nature, 374, 623
———. 1996b, in Proc. Third Compton Symp., A&AS Special Issue, in press
Novikov, I. D., & Thorne, K. S. 1973, in Blackholes, ed. C. DeWitt & B. DeWitt (New York: Gordon and Breach), 343
Pacholczyk, A. G. 1970, Radio Astrophysics, (San Francisco: Freeman)
Phinney, E. S. 1981, in Plasma Astrophysics, ed. T. D. Guyenne & G. Levy (ESA SP-161), 337
Piran, T. 1978, ApJ, 221, 652
Pringle, J. E., Rees, M. J., & Pacholczyk, A. G. 1973, A&A, 29, 179
Rees, M. J., Begelman, M. C., Blandford, R. D., & Phinney, E. S. 1982, Nature, 295, 17
Rybicki, G. B., & Lightman, A. P. 1979, Radiative Processes in Astrophysics (New York: Wiley)
Shakura, N. I., & Sunyaev, R. A. 1973, A&A, 24, 337
Shapiro, S. L., Lightman, A. P., & Eardley, D. M. 1976, ApJ, 204, 187
Stepney, S., & Guilbert, P. W. 1983, MNRAS, 204, 1266
Svensson, R. 1982, ApJ, 258, 335
———. 1984, MNRAS, 209, 175
Tanaka, Y. 1989, in Proc. 23rd ESLAB Symp. on Two Topics in X-Ray Astronomy, ed. J. Hunt & B. Battrick (ESA SP-296), 3
Wandel, A., & Liang, E. P. 1991, ApJ, 380, 84
White, T. R., & Lightman, A. P. 1989, ApJ, 340, 1024